

Evaluation of UV-fs-LA-MC-ICP-MS for Precise *in situ* Copper Isotopic Microanalysis of Cubanite

Kei IKEHATA*[†] and Takafumi HIRATA**

*Faculty of Life and Environmental Sciences, University of Tsukuba, 1-1-1 Tennodai, Tsukuba, Ibaraki 305-8572, Japan

**Division of Earth and Planetary Sciences, Graduate School of Science, Kyoto University, Kitashirakawa Oiwakecho, Sakyo, Kyoto, Kyoto 606-8502, Japan

We evaluated the capabilities of an *in situ* method for measuring copper isotopes of cubanite using UV-fs-LA-MC-ICP-MS. A comparison of the UV-fs laser results with those obtained from the NIR-fs laser system shows that there is obviously an improvement in the precision (<0.10%, 2SE) when using the UV-fs laser. In both wavelength modes, matrix-matched standards are required for reliable *in situ* copper isotope analysis of cubanite. This method was applied to determinations for copper isotopes of minute cubanite grains in a skarn ore. Copper isotopic ratios of cubanite grains near a weathered surface of the sample are lower than those of intact cubanite grains within the sample, suggesting that selective leaching of heavier copper isotope in primary minerals occurred during weathering.

Keywords Copper isotope, cubanite, ultraviolet, near-infrared, femtosecond laser, MC-ICP-MS

(Received June 29, 2013; Accepted October 8, 2013; Published December 10, 2013)

Introduction

Recent advances in multiple collector inductively coupled plasma mass spectrometry (MC-ICP-MS) have made it possible to determine isotopic variations of non-traditional stable isotopes, such as copper, iron and zinc in natural samples with high precision and accuracy.¹ Copper has two stable isotopes, ⁶³Cu and ⁶⁵Cu. Previous copper isotope measurements of copper-rich minerals from various environments have revealed a significantly large variation in the $\delta^{65}\text{Cu}$ values from -16.5 to 10.0‰, relative to the NIST-SRM976 standard.² This variation is quite large compared with other non-traditional stable isotopes (e.g., Fe and Zn),¹ presumably due to significant isotope fractionations during redox reactions (oxidation states 0, +1 and +2 of Cu are not uncommon in nature, compared with Fe and Zn) that occurred at relatively low temperatures.¹⁻¹⁴ Therefore, the copper isotopes are potentially an excellent tracer of geological and biological processes.

Cubanite is a common sulfide mineral of iron and copper (CuFe₂S₃); the oxidation number of copper in CuFe₂S₃ is +1.¹⁵ Cubanite is generally complexly intergrown with other sulfide minerals, or very fine grained in nature. Therefore, the sampling of specific minerals could be very difficult. The laser ablation (LA)-ICP-MS technique allows us to measure the copper isotopic ratios in cubanite with high spatial resolution. Recently, femtosecond (fs) laser ablation systems with short pulse widths have become available. The use of femtosecond ablation drastically reduces or eliminates thermal-induced isotope fractionation that may occur during the laser ablation of metal,

sulfide and oxide minerals using conventional nanosecond (ns) pulsed laser ablation systems, and thus improving the analytical precision and accuracy of iron and copper isotopes compared to nanosecond laser ablation.^{16,17} Horn *et al.*¹⁶ reported that ultraviolet (UV)-fs-LA-MC-ICP-MS analyses did not require matrix-matched standards to obtain reliable iron isotope ratios of many iron-rich materials. In contrast, matrix-matched standards were still required for reliable *in situ* copper isotope analyses of copper-iron sulfide minerals (chalcocite and chalcopyrite) by using near-infrared (NIR)-fs-LA-MC-ICP-MS.¹⁷ Although large well-crystallized cubanite is extremely rare, recently several natural crystals of cubanite appropriate for standards of laser analysis were obtained. In this study, we evaluated an *in situ* method for determining the copper isotopic composition of cubanite using UV-fs-LA-MC-ICP-MS with a laser spot diameter of 15 μm , and compared the analytical performance of the UV-fs- and NIR-fs-laser system. The method was then applied to measurements of the copper isotopic ratios of cubanite in a skarn deposit from the Mihara mine, Japan in order to investigate the variability of copper isotopic compositions in cubanite within a cubanite-bearing ore.

Experimental

Samples, standard and sample preparations

The four cubanite samples used for the experiments were from the Henderson No. 2 mine, Chibougamau, Canada (Cb-1 and Cb-2) and from the Morro Velho mine, Nova Lima, Brazil (Cb-3 and Cb-4). A NIST-SRM 976 (National Institute of Standards and Technology, USA) metallic copper disc was used as a reference copper isotopic standard. Cubanite samples were broken into small fragments using an agate mortar. Optically

[†] To whom correspondence should be addressed.
E-mail: ikkei@geol.tsukuba.ac.jp

pure mineral fragments were selected and hand-picked under a binocular microscope. All fragments showing alteration, cracks and fractures were removed during handpicking. Phase identification and the determination of major and minor element compositions (Cu, Fe, Co, Ni, Zn, As and S) of samples were carried out using a reflected light microscope and an electron probe microanalyzer (EPMA, JEOL JXA-8530F) at the Chemical Analysis Division, University of Tsukuba. In order to evaluate the accuracy of the laser ablation technique, the selected fragments (except for the largest Cb-1 crystal) were divided into two aliquots; one was used for solution MC-ICP-MS analysis, and the other for laser ablation MC-ICP-MS analysis. The Cb-1 crystal was divided into five parts: two (Cb-1A) were used for laser ablation and solution MC-ICP-MS analyses, and the others (Cb-1B, Cb-1C and Cb-1D) for solution MC-ICP-MS analysis to verify the copper isotope homogeneity of the Cb-1 crystal. The aliquots of samples used for laser ablation analysis were embedded into epoxy mounts, and then polished to a 1- μm finish. The other aliquots for solution analysis were dissolved by aqua regia in Teflon beakers on a hotplate, and then evaporated to dryness. The resulting sample residues were redissolved in 0.5% nitric acid, and diluted to 100 ppm Cu for a stock solution. Every analyzed solution (200 ppb Cu in 0.1% nitric acid) was prepared by dilution of the stock solution.

For solution samples, a number of previous studies evaluated the matrix effects of iron and sulfur on copper isotope measurements, and demonstrated that, within the error ($<0.10\%$, 2σ), there were no resolvable matrix effects on the copper isotope ratios, even in samples with high Fe/Cu (<15) and S/Cu (<10) ratios.^{4,7,17} To evaluate the matrix effects of iron and sulfur on our copper isotope analyses, we added iron and sulfur at concentrations higher than in the cubanite samples (Fe/Cu > 2 ; S/Cu > 3) to a NIST-SRM 976 solution. The resulting $^{65}\text{Cu}/^{63}\text{Cu}$ ratios did not vary measurably ($<0.06\%$), suggesting a very small level of the matrix effects. Thus, anion-exchange chromatography was not applied to purify the sample solutions in this study.

Apparatus and analytical methods for copper isotope analyses

Copper isotope analyses were performed on a Nu Plasma 500 MC-ICP-MS (Nu Instruments, Wrexham, UK) at the Division of Earth and Planetary Sciences, Kyoto University.^{12-14,17} A standard-sample-standard bracketing technique was applied to correct the instrumental mass fractionation and drift. The detailed operating conditions for both solution and laser analyses are presented in Table 1.

For the solution sample, the sample was introduced into the ICP through nebulization using a MicroMist 100 (Glass Expansion, Melbourne, Australia), and sample uptake rate was $150 \mu\text{L min}^{-1}$. Data were collected with 20 integrations of 5 s each, in blocks of 3. Baselines were measured before each block for 30 s at half-mass at the low-mass side of the peak. For *in situ* copper isotope analyses, the MC-ICP-MS was coupled to a titanium:sapphire femtosecond laser ablation system (IFRIT, Cyber Laser Inc., Japan) operating in the fundamental NIR wavelength range (780 nm) and UV wavelength range (260 nm) by third-harmonic generation. The laser was operated at a pulse energy ranging from 5 to 20 μJ , with a repetition rate ranging from 5 to 15 Hz, obtaining constant total signal intensities (7 - 10 V) of copper. For each sample, copper isotope analyses of 5 to 7 spots were made with 10 s integration times for each spot; the washout time between spots was *ca.* 20 s. All copper isotope ratios are presented in a standard delta ($\%$) notation, which is defined as

Table 1 Typical operating conditions for the MC-ICP-MS and laser ablation system

MC-ICP-MS:	Nu Plasma 500 (Nu Instruments, UK)
ICP ion source:	
ICP	27.12 MHz
Rf forward power	1350 W
Rf reflected power	<1 W
Coolant gas flow	13.0 L min^{-1}
Auxiliary gas flow	0.7 L min^{-1}
Nebulizer gas flow	<i>ca.</i> 1.0 L min^{-1}
Mass spectrometer:	
Ion energy	4000 V
Extraction	2400 V
Analysis mode	Static
Collector configuration	L2 (^{63}Cu), H2 (^{65}Cu)
Nebulizer:	MicroMist 100 (Glass Expansion, Australia)
Uptake rate	$150 \mu\text{L min}^{-1}$
Spray chamber	Glass cyclonic type
Analysis protocol:	
Acquisition mode	Time resolved analysis (TRA)
Analysis duration	Solution: 30 s background, 5 s integration time Laser: 30 s background, 10 s ablation
Laser ablation system:	Cyber Probe IFRIT (Cyber Laser Inc., Japan) Titanium:sapphire femtosecond laser
Laser parameter:	
Wavelength	NIR (780 nm), UV (260 nm)
Pulse width	227 fs
Ablation mode	Single spot
Spot diameter	15 μm
Pulse energy	5 - 20 μJ
Repetition rate	5 - 15 Hz
Carrier gas flow:	He: 0.6 L min^{-1} , Ar: <i>ca.</i> 1.0 L min^{-1}
Preablation:	None
Tube length:	<i>ca.</i> 4.0 m
Pulse smoothing manifold:	<i>ca.</i> 150 cm^3 (Baffled Type)

$$\delta^{65}\text{Cu} = [(R_{\text{sample}}/R_{\text{std}}) - 1] \times 1000, \quad (1)$$

where R_{sample} is the measured $^{65}\text{Cu}/^{63}\text{Cu}$ ratio for the unknown sample and R_{std} the mean $^{65}\text{Cu}/^{63}\text{Cu}$ ratio of the NIST-SRM976 standard.

Matrix-matched standards were required for reliable *in situ* copper isotope analysis of copper-iron sulfide minerals by using NIR-fs-LA-MC-ICP-MS.¹⁷ Therefore, in order to evaluate the possible matrix effects on our LA-MC-ICP-MS analyses, a matrix-matched mineral standard was also used in place of the NIST-SRM 976 copper standard. Because certified cubanite standards for copper isotope analysis were not available, we used the Cb-1A as our in-house cubanite matrix-matched standard, after determining their copper isotope ratios by means of a conventional solution nebulization MC-ICP-MS technique (see the following chapter for details).

Results and Discussion

Evaluation for *in situ* measurement of copper isotopes of cubanite

Major element compositions of the cubanite grains are given in Table 2. The results for both the solution and laser ablation copper isotope analyses of the cubanite samples are summarized in Table 2 and Fig. 1. The Cb-1A, Cb-2, Cb-3 and Cb-4 grains for laser ablation analyses have nearly stoichiometric chemical

Table 2 Comparison of solution and laser ablation copper isotope analyses for the cubanite samples

Sample	Locality	Major element compositions ^a			Solution analyses	Laser analyses (NIR)		Laser analyses (UV)	
		Cu, wt%	Fe, wt%	S, wt%	$\delta^{65}\text{Cu}$, ‰ ^b	$\delta^{65}\text{Cu}$, ‰ ^b	$\delta^{65}\text{Cu}$, ‰ ^c	$\delta^{65}\text{Cu}$, ‰ ^b	$\delta^{65}\text{Cu}$, ‰ ^c
Cb-1A	Henderson No. 2 mine	22.7 ± 0.25 (n = 5)	41.1 ± 0.14 (n = 5)	35.3 ± 0.14 (n = 5)	0.00 ± 0.05 (n = 6)	0.56 ± 0.18 (n = 7)		0.76 ± 0.10 (n = 7)	
Cb-1B	Henderson No. 2 mine				0.02 ± 0.02 (n = 4)				
Cb-1C	Henderson No. 2 mine				-0.01 ± 0.06 (n = 4)				
Cb-1D	Henderson No. 2 mine				-0.03 ± 0.03 (n = 4)				
Cb-2	Henderson No. 2 mine	22.6 ± 0.16 (n = 5)	41.2 ± 0.14 (n = 5)	35.2 ± 0.54 (n = 5)	0.36 ± 0.05 (n = 6)		0.34 ± 0.19 (n = 5)	1.08 ± 0.10 (n = 7)	0.36 ± 0.10 (n = 5)
Cb-3	Morro Velho mine	22.5 ± 0.43 (n = 5)	41.4 ± 0.48 (n = 5)	35.1 ± 0.55 (n = 5)	0.03 ± 0.05 (n = 5)		0.03 ± 0.15 (n = 5)	0.77 ± 0.10 (n = 5)	-0.02 ± 0.09 (n = 5)
Cb-4	Morro Velho mine	22.6 ± 0.28 (n = 5)	41.3 ± 0.37 (n = 5)	35.0 ± 0.43 (n = 5)	-0.09 ± 0.08 (n = 5)		-0.10 ± 0.17 (n = 6)	0.69 ± 0.09 (n = 5)	-0.11 ± 0.08 (n = 6)

a. The data determined by EPMA. Other detected element is only cobalt (<0.08 wt%). b. The data corrected using the NIST-SRM976 copper standard. c. The data corrected for matrix effects by using the matrix-matched standards (Cb-1A). The errors are analytical precision of individual analysis at the 2 σ level.

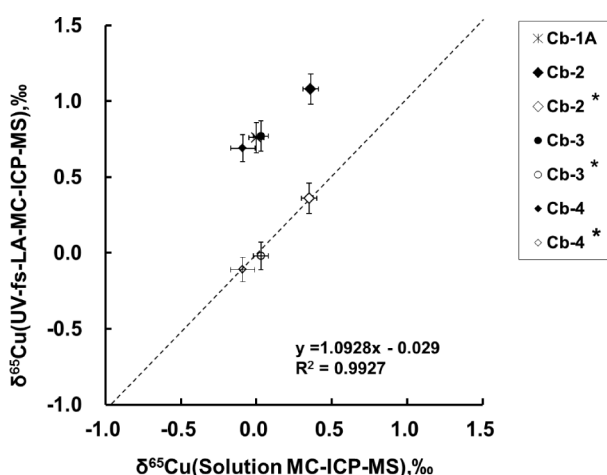


Fig. 1 Comparison of the $\delta^{65}\text{Cu}$ values for cubanite samples measured by solution MC-ICP-MS and by UV-fs-LA-MC-ICP-MS. The error bars represent the analytical precision of individual analysis at the 2 σ level. The dotted line shows the regression line of all data corrected for matrix effects; * is the data corrected for matrix effects using the Cb-1A as the cubanite calibrating standard.

composition (CuFe_2S_3) with minor amounts of cobalt. The $\delta^{65}\text{Cu}$ values of the Cb-1A, Cb-1B, Cb-1C and Cb-1D grains measured by solution MC-ICP-MS are essentially identical within the error, indicating that the Cb-1A ($\delta^{65}\text{Cu} = 0.00 \pm 0.05\text{‰}$) is suitable for our in-house cubanite matrix-matched standard. Concerning the laser (NIR mode) ablation result of the Cb-1A, the average $\delta^{65}\text{Cu}$ value, relative to the NIST-SRM 976 standard, is $0.56 \pm 0.18\text{‰}$, which is significantly higher than the solution nebulization value of $0.00 \pm 0.05\text{‰}$. The laser (NIR mode) analyses on the Cb-2, Cb-3 and Cb-4, using the Cb-1A as a cubanite in-house standard, give average $\delta^{65}\text{Cu}$ values of $0.34 \pm 0.19\text{‰}$, $0.03 \pm 0.15\text{‰}$ and $-0.10 \pm 0.17\text{‰}$. These are identical to solution results of $0.36 \pm 0.05\text{‰}$, $0.03 \pm 0.05\text{‰}$ and $-0.09 \pm 0.08\text{‰}$, respectively. Laser analyses (UV mode) for the Cb-1A, Cb-2, Cb-3 and Cb-4 yield respective average $\delta^{65}\text{Cu}$ values of $0.76 \pm 0.10\text{‰}$, $1.08 \pm 0.10\text{‰}$, $0.77 \pm 0.10\text{‰}$ and

$0.69 \pm 0.09\text{‰}$ when calibrated against the NIST-SRM 976 standard. These values are systematically higher than the solution nebulization values of $0.00 \pm 0.05\text{‰}$, $0.36 \pm 0.05\text{‰}$, $0.03 \pm 0.05\text{‰}$ and $-0.09 \pm 0.08\text{‰}$, respectively. The laser analyses (UV mode) on the Cb-2, Cb-3 and Cb-4, using the Cb-1A in-house standard, give average $\delta^{65}\text{Cu}$ values of $0.36 \pm 0.10\text{‰}$, $-0.02 \pm 0.09\text{‰}$ and $-0.11 \pm 0.08\text{‰}$, respectively. These are indistinguishable within the measurement uncertainty from the solution results.

It has been demonstrated that precise copper isotopic ratios of cubanite can be obtained from all samples using the fs-LA-MC-ICP-MS (NIR and UV mode) and standard-sample-standard bracketing technique, comparable to previously reported copper isotope results of copper-rich materials using NIR-fs-LA-MC-ICP-MS.¹⁷ A comparison of the UV-fs laser results with those obtained from the NIR-fs laser system shows that there is obviously an improvement in the precision when using the UV-fs laser. This tendency is similar to a previous result, that the use of short laser wavelengths reduces the production of larger particles (signal spikes) from a laser pit in ns-LA-ICP-MS, and therefore improves the analytical precision compared to long wavelengths.¹⁸ Despite relatively good analytical precision, the discrepancies between the copper isotopic compositions obtained by LA-MC-ICP-MS and solution MC-ICP-MS for cubanite samples were observed when the NIST-SRM 976 standard was adopted as the bracketing standard. For laser ablation measurements of cubanite samples, accurate copper isotopic data can be obtained using a matrix-matched calibrating standard (Cb-1A) of similar composition to the other cubanite samples. The poor accuracy of the laser results of cubanite samples may be attributed to the difference in the chemical compositions, or physicochemical features between the NIST-SRM 976 metallic copper standard and sample materials (cubanite in this study). Previous studies also showed that highly reliable copper isotopic measurements of copper-iron sulfide minerals (chalcocite and chalcopyrite) could be achieved by ns- and fs-LA-MC-ICP-MS analyses, when the data were calibrated using a matrix-matched standard,^{17,19} though Horn *et al.*¹⁶ reported that UV-fs-LA-MC-ICP-MS analyses did not require matrix-matched standards to obtain precise and reliable

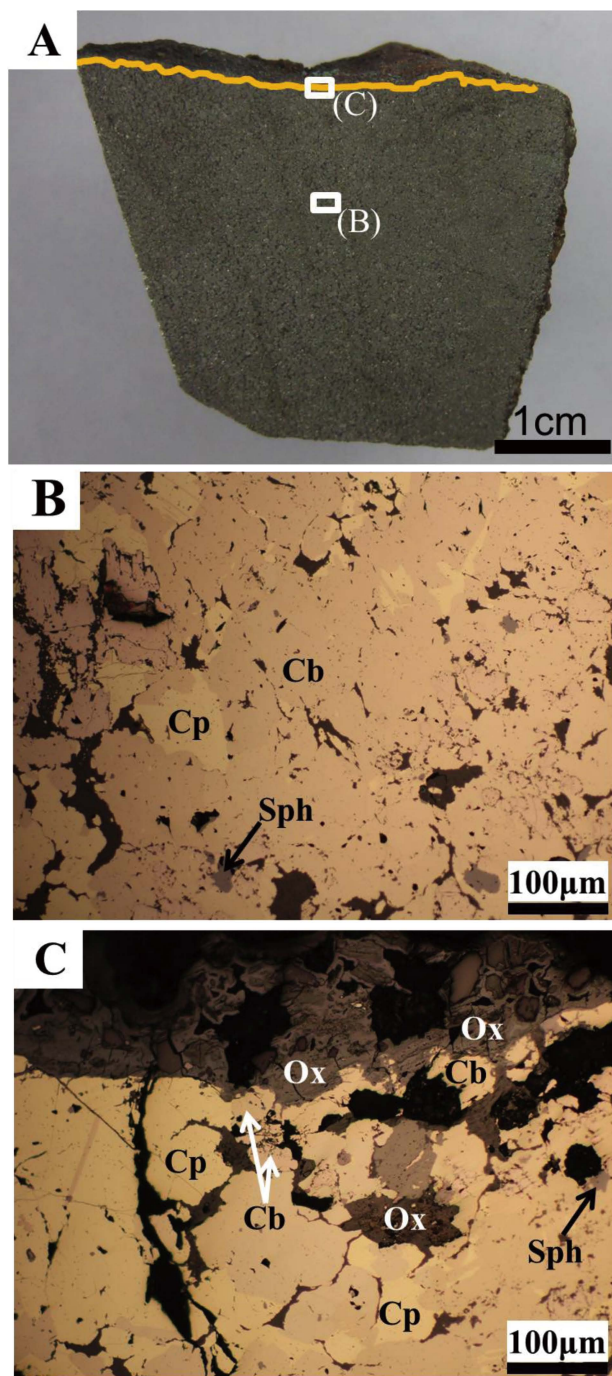


Fig. 2 Photographs of a cubanite-bearing massive sulfide ore from the Mihara mine, Okayama, Japan. A, Photograph of the cutting surface of the ore. The surface of the sample comprises thin secondary iron and copper minerals (*e.g.*, malachite) formed by low-temperature surface oxidation or weathering of primary sulfide minerals. Copper isotopic ratios of cubanite grains located near weathered surfaces of the sample (orange-colored band) are lower than those dispersed near the center of the sample. The areas (B and C) enclosed by a rectangle are enlarged in (B) and (C). B, Reflected light photomicrograph of primary fine-grained cubanite (Cb) grains dispersed near the center of the sample. Other sulfide minerals are chalcopyrite (Cp), with lesser amounts of sphalerite (Sph) and pyrrhotite. C, Reflected light photomicrograph of primary fine-grained cubanite (Cb) grains located in immediate proximity to the outermost secondary oxide or hydroxide minerals (Ox) formed by low-temperature surface oxidation or the weathering of primary sulfide minerals. Other sulfide minerals are chalcopyrite (Cp), with lesser amounts of sphalerite (Sph) and pyrrhotite.

iron isotope ratios of iron-rich materials. Therefore, careful selections of standards are required for accurate *in situ* copper isotope analysis of copper-bearing minerals.

Application to cubanite micro-grains from the Mihara mine, Japan

The UV-fs-LA-MC-ICP-MS technique was applied to measurements for copper isotopes of cubanite grains in an ore collected from a dump in the abandoned Mihara mine located in Yoshii-cho, Ibara City, Okayama Prefecture, Japan. The mine is a high-temperature skarn deposit of copper, embedded in Paleozoic limestone.²⁰ The collected sample was a massive sulfide ore composed mainly of primary fine-grained cubanite and chalcopyrite, with lesser amounts of sphalerite and pyrrhotite (Figs. 2A and 2B). The surface of the sample comprised thin secondary iron and copper minerals (*e.g.*, malachite), formed by low-temperature surface oxidation or the weathering of primary sulfide minerals (Figs. 2A and 2C).

Major element compositions and copper isotopic ratios of the cubanite grains are given in Table 3. Cubanite grains dispersed near the center of the sample represent significantly pure chemical compositions (Cu = 22.6 ± 0.20 wt%, Fe = 41.4 ± 0.13 wt%, S = 35.3 ± 0.57 wt%; 2σ , $n = 10$). They have $\delta^{65}\text{Cu}$ values of between 0.19 and 0.28‰. Cubanite grains located in immediate proximity to the outermost secondary iron and copper minerals also have significantly pure chemical compositions (Cu = 22.6 ± 0.21 wt%, Fe = 41.5 ± 0.11 wt%, S = 35.3 ± 0.37 wt%; 2σ , $n = 10$). However their $\delta^{65}\text{Cu}$ values range from -0.01 to 0.05‰, and are obviously lighter than those of other cubanite grains within the hand specimen, though the compositional differences among cubanite in the sample detected by EPMA are significantly small (Table 3).

Our copper isotopic results (patterns) concerning cubanite grains within a single sample are in agreement with previous observations of secondary ore deposits, and the results of leaching experiments; *i.e.*, selective preferential oxidation or leaching of the heavier copper isotope in primary copper minerals occurs during low-temperature oxidation (weathering) processes. Therefore, a comparison of the $\delta^{65}\text{Cu}$ values of coexisting primary copper-rich minerals (Cu(I)) and secondary copper-rich minerals (Cu(II)) within a single sample shows that secondary copper-rich minerals (Cu(II)) are enriched in ^{65}Cu relative to primary copper-rich minerals (Cu(I)).¹⁻¹⁴ As a result, the residual primary copper-rich minerals (Cu(I)) have their $\delta^{65}\text{Cu}$ values shifted toward lower values as the leaching processes proceed.¹⁻¹⁴ In the case of our sample, primary cubanite grains near the weathered surface of the sample were significantly affected by dissolution during low-temperature oxidation and weathering processes, and copper (Cu(I)) in the cubanite grains was probably leached, and precipitated as thin secondary minerals (malachite) (Cu(II)). Thus, these grains show lower $\delta^{65}\text{Cu}$ values than intact cubanite grains dispersed near the center of the sample. Our results demonstrate the capabilities of the UV-fs-LA-MC-ICP-MS technique applied to cubanite copper isotopic systematics for ore mineralogy.

Acknowledgements

This research was partly supported by a Grant-in-Aid for Scientific Research from the Ministry of Education, Culture, Sports, Science and Technology, Japan, and the Chemical Analysis Division 2012 Research Grant from the Research Facility Center for Science and Technology, University of Tsukuba. Dr. T. Iizuka and an anonymous reviewer are thanked

Table 3 Major and trace element compositions and copper isotopic ratios of cubanite grains in the sulfide ore from the Mihara mine, Japan

Grain No.	Location of cubanite in the sample	Major and trace element composition ^a							Copper isotopic ratio ^b
		Cu, wt%	Fe, wt%	Co, wt%	Ni, wt%	Zn, wt%	As, wt%	S, wt%	$\delta^{65}\text{Cu}$, ‰
M-1	Central part	22.6	41.4	0.05	b.d.l.	0.05	b.d.l.	35.0	0.21
M-2	Central part	22.6	41.4	0.07	b.d.l.	b.d.l.	b.d.l.	35.1	0.23
M-3	Central part	22.7	41.4	0.07	b.d.l.	0.07	b.d.l.	35.5	0.20
M-4	Central part	22.6	41.4	0.09	b.d.l.	b.d.l.	b.d.l.	35.3	0.26
M-5	Central part	22.4	41.4	0.06	b.d.l.	b.d.l.	b.d.l.	35.4	0.27
M-6	Central part	22.5	41.5	0.10	b.d.l.	0.06	b.d.l.	35.3	0.25
M-7	Central part	22.6	41.5	0.10	b.d.l.	b.d.l.	b.d.l.	34.7	0.28
M-8	Central part	22.7	41.5	0.08	b.d.l.	b.d.l.	b.d.l.	35.6	0.24
M-9	Central part	22.6	41.3	0.10	b.d.l.	b.d.l.	b.d.l.	35.5	0.27
M-10	Central part	22.8	41.4	0.05	b.d.l.	b.d.l.	b.d.l.	35.5	0.19
M-11	Outermost part	22.7	41.5	0.10	b.d.l.	b.d.l.	b.d.l.	35.3	0.04
M-12	Outermost part	22.5	41.5	b.d.l.	b.d.l.	0.05	b.d.l.	35.3	0.01
M-13	Outermost part	22.5	41.4	0.08	b.d.l.	b.d.l.	b.d.l.	35.1	0.02
M-14	Outermost part	22.7	41.5	0.07	b.d.l.	0.05	b.d.l.	35.0	0.05
M-15	Outermost part	22.6	41.5	b.d.l.	b.d.l.	b.d.l.	b.d.l.	35.5	0.03
M-16	Outermost part	22.5	41.5	b.d.l.	b.d.l.	0.07	b.d.l.	35.1	0.01
M-17	Outermost part	22.5	41.5	b.d.l.	b.d.l.	0.08	b.d.l.	35.2	-0.01
M-18	Outermost part	22.6	41.5	b.d.l.	b.d.l.	0.08	b.d.l.	35.4	0.03
M-19	Outermost part	22.7	41.4	b.d.l.	b.d.l.	b.d.l.	b.d.l.	35.3	0.03
M-20	Outermost part	22.4	41.5	0.07	b.d.l.	0.07	b.d.l.	35.5	0.02

a. The data determined by EPMA. b. The data determined by UV-fs-LA-MC-ICP-MS. b.d.l. = below detection limit of the EPMA (<0.05 wt%).

for their constructive comments that helped improve the manuscript.

References

1. C. M. Johnson, B. L. Beard, and F. Albarède, "Geochemistry of non-traditional stable isotopes", **2004**, Vol. 55, Rev. Mineral, Mineral. Soc. America, Washington, D.C.
2. R. Mathur, S. Titley, F. Barra, S. Brantley, M. Wilson, A. Phillips, F. Munizaga, V. Maksae, J. Vervoort, and G. Hart, *J. Geochem. Explor.*, **2009**, 102, 1.
3. C. N. Maréchal, P. Télouk, and F. Albarède, *Chem. Geol.*, **1999**, 156, 251.
4. X. K. Zhu, R. K. O'Nions, Y. Guo, N. S. Belshaw, and D. Rickard, *Chem. Geol.*, **2000**, 163, 139.
5. P. B. Larson, K. Maher, F. C. Ramos, Z. Chang, M. Gaspar, and L. D. Meinert, *Chem. Geol.*, **2003**, 201, 337.
6. O. Rouxel, Y. Fouquet, and J. N. Ludden, *Econ. Geol.*, **2004**, 99, 585.
7. S. Graham, N. Pearson, S. Jackson, W. Griffin, and S. Y. O'Reilly, *Chem. Geol.*, **2004**, 207, 147.
8. R. Mathur, J. Ruiz, S. Titley, L. Liermann, H. Buss, and S. Brantley, *Geochim. Cosmochim. Acta*, **2005**, 69, 5233.
9. G. Markl, Y. Lahaye, and G. Schwinn, *Geochim. Cosmochim. Acta*, **2006**, 70, 4215.
10. D. Asael, A. Matthews, S. Oszczepalski, M. Bar-Matthews, and L. Halicz, *Chem. Geol.*, **2009**, 262, 147.
11. B. E. Kimball, R. Mathur, A. C. Dohnalkova, A. J. Wall, R. L. Runkel, and S. L. Brantley, *Geochim. Cosmochim. Acta*, **2009**, 73, 1247.
12. K. Ikehata, Ph.D. Thesis, The University of Tokyo, Tokyo, **2009**.
13. K. Ikehata, K. Notsu, and T. Hirata, *Econ. Geol.*, **2011**, 106, 307.
14. K. Ikehata and T. Hirata, *Econ. Geol.*, **2012**, 107, 1489.
15. S. W. Goh, A. N. Buckley, W. M. Skinner, and L.-J. Fan, *Phys. Chem. Miner.*, **2010**, 37, 389.
16. I. Horn, F. von Blanckenburg, R. Schoenberg, G. Steinhoefel, and G. Markl, *Geochim. Cosmochim. Acta*, **2006**, 70, 3677.
17. K. Ikehata, K. Notsu, and T. Hirata, *J. Anal. At. Spectrom.*, **2008**, 23, 1003.
18. M. Guillong, I. Horn, and D. Günther, *J. Anal. At. Spectrom.*, **2003**, 18, 1224.
19. W. Li, S. E. Jackson, N. J. Pearson, and S. Graham, *Geochim. Cosmochim. Acta*, **2010**, 74, 4078.
20. A. Soeda, *Mining Geol.*, **1960**, 10, 346.